CrystEngComm

Accepted Manuscript

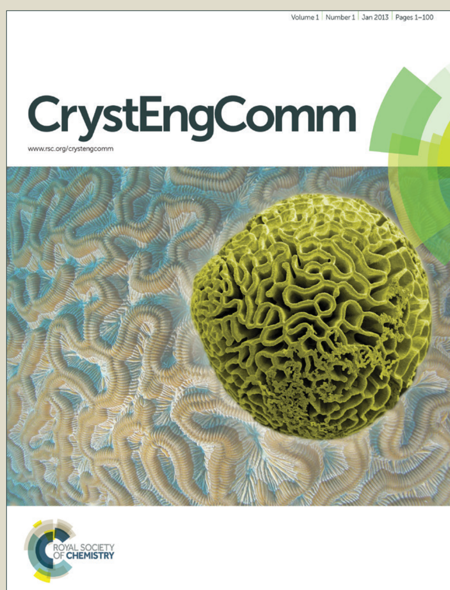

This is an *Accepted Manuscript*, which has been through the Royal Society of Chemistry peer review process and has been accepted for publication.

Accepted Manuscripts are published online shortly after acceptance, before technical editing, formatting and proof reading. Using this free service, authors can make their results available to the community, in citable form, before we publish the edited article. We will replace this *Accepted Manuscript* with the edited and formatted *Advance Article* as soon as it is available.

You can find more information about *Accepted Manuscripts* in the Information for Authors.

Please note that technical editing may introduce minor changes to the text and/or graphics, which may alter content. The journal's standard Terms & Conditions and the Ethical guidelines still apply. In no event shall the Royal Society of Chemistry be held responsible for any errors or omissions in this *Accepted Manuscript* or any consequences arising from the use of any information it contains.

ROYAL SOCIETY OF CHEMISTRY

www.rsc.org/crystengcomm

Epitaxial growth mechanism of pulsed laser deposited AlN films on Si (111) substrates

Hui Yang,[a] Wenliang Wang,[a] Zuolian Liu,[a] Weijiang Yang [a] and Guoqiang Li [a, b *]

[a]State Key Laboratory of Luminescent Materials and Devices, South China University of Technology, Guangzhou 510640, China

[b]Department of Electronic Materials, School of Materials Science and Engineering, South China University of Technology, Guangzhou 510640, China

[*]Corresponding author, E-mail: msgli@scut.edu.cn

Abstract

The epitaxial growth mechanism and dislocations formation causes of AlN films on Si substrate by pulsed laser deposition (PLD) are comprehensively proposed. Due to the highly energetic effect and pulsed effect of PLD, the epitaxial process of AlN film growing on Si (111) by PLD is two-dimensional layer-by-layer growth regime in relation to strain-relaxation mechanisms. The three PLD sub-stages of epitaxial process for AlN films on Si substrate have been suggested and interpreted in detail. At the optimum growth conditions, it exhibits 1.5 nm-thick single-crystalline AlN interfacial layers with high density of dislocations, rather than an amorphous SiN_x layer. In the contrary, severely interfacial reaction and an AlSiN layer were found in the AlN/Si (111) interface in non-optimal growth conditions, which is derived from the interfacial interdiffusion and penetration between active Si atoms and AlN species, resulting in high density of dislocations and defects in AlN/Si (111) interface.

Keywords: growth mechanism; layer-by-layer; interfacial layer; pulsed laser deposition; dislocations

1. Introduction

CrystEngComm Accepted Manuscript

Aluminum nitride (AlN) has wide band gap (6.2 eV), high surface acoustic wave velocity (5760 m/s), high thermal conductivity, and good thermal stabilities.[1-3] These properties make AlN important for applications in electronic and optoelectronic devices, such as deep ultraviolet (DUV) light emitting diode, short wavelength emitters, telecommunication filters, and bulk acoustic wave resonators (FBARs), etc.[4-6] In order to realize the integration of AlN related devices, epitaxial growth of AlN on Si substrate has become a primary requirement for these applications.[7,8]

However, it is not easy to epitaxially grow AlN on Si. Apart from high density of dislocations in the grown AlN films due to the large lattice mismatch with Si, another main difficulty is the stress induced by the thermal expansion mismatch that leads to cracks in AlN epilayers.[9,10] Various techniques have been reported for the epitaxial growth of AlN films on Si substrates. These include metal-organic chemical vapor deposition (MOCVD), [11] plasma-assisted molecular beam epitaxy (MBE),[12] and pulsed laser deposition (PLD).[13] Among them, PLD employs a highly energetic pulsed laser to ablate targets, so as to assure high kinetic energy of species when arriving substrates, and therefore realize the epitaxial growth of single-crystalline at a relatively low growth temperature and with an abrupt interface.[14-15]

Usually, the PLD process from most theoretical models can be categorized into three sub-stages as (i) laser ablation and interaction with target, (ii) plasma plume expansion into a background gas, and （iii）thin film deposition at the substrate.[16-18] In the PLD process, the initial ablation process includes laser radiation penetrates inside target, evaporates and ionizes the target material, creating a plasma plume above the target surface. Subsequently, atoms, molecules, and ions of react plasma plume collide and with background gas, leading highly directional expansion species perpendicular to the target. Finally, plasma species arrive at substrates in a certain kinetic energy, then undergo some different growth periods and eventually a film forms on the substrates. These PLD processes have been investigated by scientific community through theoretical simulations during last years.[19-21] Although there are some experimental analysis on the influence of one or two PLD parameters on morphology or crystal quality of AlN films grown on Si substrate, [22-23] one can hardly find any report on the thorough investigation of inherent epitaxial mechanism underlying the three PLD growth processes of AlN films on Si substrate by PLD. In this work, we report on a comprehensive study of epitaxial growth mechanism and dislocation formation causes of AlN films on Si (111) substrates by PLD.

CrystEngComm Accepted Manuscript

2. Experimental

The depositions of AlN on Si (111) substrates were performed in an ultra-high vacuum (UHV) pulsed laser deposition chamber with KrF excimer laser (λ=248 nm, t=20 ns). The Si (111) substrates were chemically cleaned by H_2SO_4:H_2O_2:H_2O (3:1:1) and 5% HF before loaded into the reactor. The substrates were then introduced into the UHV chamber with a background pressure of 1×10^{-10} Torr and baked at 900°C for 60 min to remove residual surface contaminations. The KrF excimer laser was used to ablate a sintered AlN target (99.99% purity) with an energy density of 2.0 J/cm^2. Subsequently, after pre-ablation of AlN target for 10 min without nitrogen plasma, AlN films were deposited under 4×10^{-4} ~ 1.2×10^{-2} Torr nitrogen (99.99999%) plasma ambient produced by the RF plasma generator for 30 min. Substrate temperature was maintained at 850 °C for the growth. The as-grown films were characterized by high-resolution x-ray diffraction (HRXRD), high-resolution transmission electron microscopy (HRTEM), scanning electron microscopy (SEM), and energy dispersive spectrometer (EDS).

3. Results

The crystalline quality of AlN films are investigated by HRXRD. Fig. 1a shows the typical ω-2θ scan curve of the as-grown films grown from 4×10^{-4} to 8×10^{-3} Torr. It shows the diffraction peaks from AlN {0001} and Si{111}, which confirms that the as-grown AlN films are single crystalline with the *c* axis normal to Si(111), AlN [0001]//Si [111]. Fig. 1b reveals the influence of nitrogen pressure on the crystalline quality of as-grown AlN films. The FWHMs of both (0002) and (10-12) XRD rocking curves of AlN films firstly decrease and then increase as the pressure increases. The FWHM of AlN (0002) rocking curve is reduced from 1.87° to 1.2° when the pressure increases from 4×10^{-4} to 8×10^{-3} Torr. However, when the pressure further increases to 1.2×10^{-2} Torr, the crystalline quality of as-grown AlN films becomes poorer. Therefore, the nitrogen pressure significantly affects crystalline quality of AlN films.

The surface morphology of the AlN films grown on Si (111) for 30 min at different nitrogen pressures was measured by SEM, as shown in Fig. 2. AlN films grown at the low nitrogen plasma pressures from 4×10^{-4} to 4×10^{-3} Torr display some non-uniformly distributed particulates in Fig. 2a-2c. In contrast, AlN film grown at 8×10^{-3} Torr has a relatively smooth surface, and neither micro-cracks nor particulates, are observed in Fig. 2d. However, if the nitrogen pressure is further increased to 1.2×10^{-2} Torr, AlN films become very rough with many small particles, Fig. 2e. Obviously, the nitrogen pressure

CrystEngComm Accepted Manuscript

also significantly affects surface morphologies of AlN films and 8×10^{-3} Torr is the optimal pressure, which has been confirmed by the atomic form microscopy measurements, with the sample grown under 8×10^{-3} Torr showing the lowest surface root mean square (RMS) roughness of 1.4 nm. The EDS line-scan analysis was performed for AlN film grown at 4×10^{-4} Torr, as shown in Fig. 2f. Some large particulates of about 1.5 μm are observed on film surface, where component contents of both N and Al are higher than elsewhere. This is mainly due to AlN species do not encounter enough collisions from appropriate nitrogen spices when the nitrogen pressure is lower than its optimal value. They are inclined to agglomerate with each other before deposited on the substrate surface, ending up with formation of clusters or particulates on as-grown AlN film surface, as shown in Fig 2a-2c. We have also checked the composition for the samples grown under optimum pressure as in Fig. 2d by EDS. It shows that these films are almost stoichiometric with Al/N close to 1.

The cross-sectional morphology of AlN/Si (111) films for 30 min was investigated by low-magnification TEM, as shown in Fig. 3. AlN films grown at 1×10^{-3} Torr and 8×10^{-3} Torr have approximate thicknesses of 63 nm and 96 nm respectively, and exhibit high density of threading dislocations which gradually stretch upward to top surface of AlN films (as white arrows labeled). Whereas, it can be clearly observed that AlN film grown at 8×10^{-3} Torr is with lower density of threading dislocations than that of 1×10^{-3} Torr, which is due to a portion of threading dislocations bend and even annihilate in the optimal pressure of 8×10^{-3} Torr.[24, 25] Using HRTEM images, we have calculated the density of threading dislocations for AlN film grown at 8×10^{3} Torr. We have found that its density of threading dislocations is reduced from $10^{10}/cm^2$ at the bottom to about $5\times10^{8}/cm^2$ near the surface.

Due to -18.9% lattice mismatches between AlN and Si, AlN lattice subjected to large tensile strain from Si lattice, leading to substantial mismatch stress in AlN/Si (111) interface during the growth. In order to release the mismatch stress, misfit dislocations generate in AlN/Si (111) interface. As the film thickness gradually increases, these interfacial misfit dislocations propagate and stretch upwards, resulting in the formation of threading dislocations. Meanwhile, the threading dislocations can bend and even annihilate in the optimal pressure of 8×10^{-3} Torr as the thickness increases. This is mainly attributed to the fact that large tensile strain of AlN lattice is gradually reduced as the thickness increases, and AlN species deposition changes from lattice non-relaxation mode to lattice relaxation mode. In this case, threading dislocations begin to bend in the horizontal direction of film and eventually annihilate, leading to lower density of threading dislocations.

In order to further study of interface layers for AlN films on Si (111), HRTEM of AlN/Si (111) films grown at 1×10^{-3} Torr and 8×10^{-3} Torr were investigated, as shown in Fig. 4a and 4b, respectively.

CrystEngComm Accepted Manuscript

AlN film grown at 8×10^{-3} Torr exhibits quite abrupt interface with Si substrate, and the interfacial layer thickness is as low as 1.5 nm, about 4-5 monolayers,[26] as shown in Fig. 4b. It reveals that the interfacial layer is a single-crystalline AlN layer with high density of dislocations, in which the lattices arrangement of 4-5 monolayers is almost similar to that of hexagonal AlN. Therefore, it is not an amorphous SiN_x layer as other researchers reported.[27-29] This is attributed to pre-ablation of AlN ceramic targets and appropriate PLD growth conditions, which can reduce the reaction probability between Si substrate and active N, and eventually inhibit Si-N interfacial reaction.

However, it is obvious that severely interfacial reaction has occurred in AlN/Si (111) interface for the film grown at 1×10^{-3} Torr, resulting in some boundaries disappearing and lattices penetration between AlN and Si atoms. We divide this interface into four segments denoted as A, B, C, and D. Each segment has its unique characteristic, as labeled in Fig. 4a. Segment A is an AlN layer with high density of dislocations. Segment B is consisted of orderly new lattices, which are taking place the positions of Si substrate atoms, and totally different from both AlN and Si atoms. We speculate that this is an AlSiN layer derived from the interfacial interdiffusion and penetration between active Si atoms and AlN species. At the low pressure of 1×10^{-3} Torr, laser-produced AlN species do not encounter enough collisions they reach substrate surface with excessive kinetic energy. These highly energetic AlN species bombard Si substrate when arriving at substrate, leading to localized Si lattices overcome their energy barriers and leave substrate with vacancies. These vacancies are filled by incident AlN species which can in further combine with Si atoms to form an AlSiN layer. In segment C, arranged Si atoms with some misfit dislocations are found in the boundaries with both segment B along [11-2] direction and Si substrate lattices on the left. Segment D is a cubic AlN layer rather than a hexagonal AlN layer, because lattices in this layer from horizontal and vertical directions are in the same size. This is mainly derived from that severely interfacial reaction has changed misfit stress in the interface,[30-31] which is beneficial for cubic AlN species to nucleate here.

Some reported an amorphous SiN_x layer was easily formed in the interface between AlN film and Si substrate, and amorphous cyclic patterns could be seen in selective area electron diffraction (SAED).[27] In our cases, the interfaces of AlN/Si (111) films grown at both 1×10^{-3} Torr and 8×10^{-3} Torr were not amorphous SiN_x layers, nor with cyclic SAED patterns, as shown in Fig.5.

SAED analysis of the interfaces between AlN films and Si substrates has been carried out to confirm the XRD results, as shown in Fig. 5. From SAED in the interfaces grown at both 1×10^{-3} Torr

CrystEngComm Accepted Manuscript

and 8×10^{-3} Torr, we obtain the epitaxial relationships between AlN film and Si (111) substrate, which are AlN (0001)//Si (111) and AlN [10-10]//Si [11-2]. Another relationship is AlN [-2110]//Si [-110] from the direction of electron diffraction, which is the same as previous reports.[23] Meanwhile, the pattern spots of AlN film grown at 8×10^{-3} Torr are much smaller compared to that of 1×10^{-3} Torr. It indicates AlN film grown at 8×10^{-3} Torr has higher crystalline-quality diffracted planes than that of 1×10^{-3} Torr, which is confirmed to the results of XRD.

4. Discussions

According to the above characterizations and three theoretical sub-stages of PLD, epitaxial growth mechanism of AlN films on Si (111) substrates by PLD can be comprehensively investigated and proposed. Detailed interpretations are given below.

The first sub-stage of AlN films grown on Si (111) substrates by PLD can be described as nanosecond laser interacts with AlN ceramics target. In our case, AlN ceramic is used as the target. The laser radiation penetrates into the AlN target, and evaporates and ionizes AlN material, creating a plasma plume above AlN target surface. After being absorbed high laser energy, AlN ceramic decomposes. Four decomposition reactions occur sequentially.[32] The reaction equations are as follows.

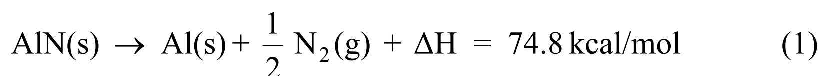

$$\mathrm{AlN(s)} \rightarrow \mathrm{Al(s)} + \frac{1}{2}\mathrm{N_2(g)} + \Delta H = 74.8\ \mathrm{kcal/mol} \quad (1)$$

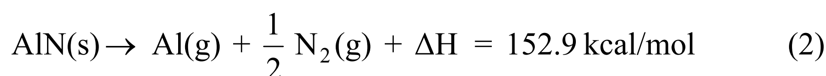

$$\mathrm{AlN(s)} \rightarrow \mathrm{Al(g)} + \frac{1}{2}\mathrm{N_2(g)} + \Delta H = 152.9\ \mathrm{kcal/mol} \quad (2)$$

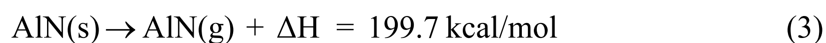

$$\mathrm{AlN(s)} \rightarrow \mathrm{AlN(g)} + \Delta H = 199.7\ \mathrm{kcal/mol} \quad (3)$$

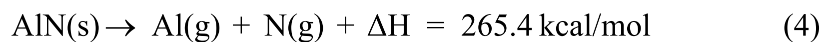

$$\mathrm{AlN(s)} \rightarrow \mathrm{Al(g)} + \mathrm{N(g)} + \Delta H = 265.4\ \mathrm{kcal/mol} \quad (4)$$

Equation (1) is the first to proceed due to its minimal reaction enthalpy. AlN ceramic target firstly decomposes into metallic Al and nitrogen, which is already found by many researchers.[33-34] They reported a low-resistivity conductive aluminum layer directly formed on AlN target surface after pulsed laser ablation. According to equations (2-4), the species decomposed by AlN ceramic are vapor phase such as Al(g), N_2(g), AlN (g), and N(g). They eventually become plasma plumes at high temperature after being absorbed higher laser energy. Thus, it is indicated that laser-ablated AlN plasma plumes include AlN, Al and N neutral species, AlN^+, Al^+ and N^+ charged species, massive electrons, etc. The same species types of plasma plumes have also investigated using time-of-flight mass spectrometry by Hai et al.[35-36] They further pointed out the density of charged species is higher than that of neutral species.

CrystEngComm Accepted Manuscript

The second sub-stage can be considered as laser-produced AlN plasma species expand into a nitrogen background. During this process, AlN plasma species collide and react with background nitrogen. Nitrogen plays an important role of acting as collision and reaction species. On the one hand, nitrogen collides with plasma species, which efficiently reduces the kinetics energy of plasma species. On the other hand, nitrogen can be excited and ionized to be N^{2+}, N^{+} and N species due to absorbing plasma energy. In ultra-high-temperature condition, ionized nitrogen species can react with Al plasma species of plume, which contributes to form stoichiometry AlN films by nitrogen incorporating into films. The complex reactions among the plasma species and background nitrogen such as excitation, ionization, dissociation and recombination, are shown as follows.[37-38]

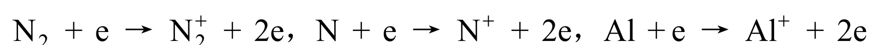

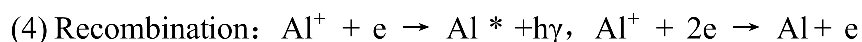

Towards the reactions involved of forming AlN, AlN^{+} and AlN species directly incorporate into AlN films. Besides, N^{2+}, N^{+} and N species can react with Al^{2+}, Al^{+} and Al species, and equally incorporate into AlN films. So nitrogen pressure is an important parameter for AlN films deposition. An appropriate nitrogen pressure in the growth chamber helps to form a stoichiometric AlN film and accordingly provide suitable kinetic energy of plasma species, which is consequently helpful for improving the surface smoothness, interface structure and crystalline quality, indicated as the optimal pressure of 8×10^{-3} Torr in Fig.2d. However, if nitrogen pressure is lower than its appropriate value, growth species will not encounter enough collisions. They reach substrate surface with excessive kinetic energy. These highly energetic species on the one hand will destruct the crystallized film and bombard Si substrate, resulting in localized Si lattices overcome the energy barrier and leave substrate with vacancies. These vacancies are filled by incident AlN species, which can in further combine with Si atoms to form an AlSiN layer, as shown in Fig. 4a. On the other hand, excessive kinetic energy leads to much collision and agglomeration among plasma species, ending up with the formation of non-uniform particulates on as-grown AlN film surface, as shown in Fig. 2a-2c.

The third one can be generalized as energetic AlN species arrive at Si substrate surface and deposit

CrystEngComm Accepted Manuscript

as AlN film. AlN film growing on Si substrate is two-dimensional layer-by-layer growth regime. We attribute this mainly to two unique effects of PLD. One is the highly energetic effect, and the other is the pulsed effect. The former effectively enhances kinetic energy of AlN species, and allow them to overcome energy barrier and rapidly migrate along scattered islands and among interlayers.[39-40] The latter enables AlN species to have enough time to adequately migrate and diffuse on Si substrate surface, and till they reach the most stable positions to deposit before next species arrive in the interrupted time of a pulse.[41-42] Both are eventually beneficial for AlN film layer-by-layer epitaxial growth on Si substrate.

In the first few pulses, energetic AlN species arrive at Si substrate surface and then diffuse and migrate adequately in the interrupted time of a pulse. When they reach the most stable positions before next species arrive, they stop as scattered growth nucleus and randomly distribute on the substrate surface.[43-45]

As PLD pulses increase, growth nucleus constantly absorb new incident species after nucleation finished and gradually become to small islands. The island density is relative to the laser energy density and laser frequency. When an energetic new specie collides with an island, the specie will transfer its energy to another specie on the island. The specie on the island received energy will take place two occasions. One occasion is that it passively leaves the island and becomes to be an independent specie which can nucleate next time. The other one is that it diffuses along this island instead of leaving, and leads to form a larger island. Moreover, due to highly energetic effect, AlN species can overcome energy barrier and rapidly diffuse among all of scattered islands.[39-40] By the way, at higher substrate temperature, AlN species diffuse much faster along scattered islands than that at low temperature. Meanwhile, the average size of islands increases as substrate temperature increase. Therefore, the highly energetic effect and substrate temperature enhancement are eventually beneficial for two-dimensional dense film growth.

When the size of large-islands increases to a certain degree, these large islands become to coalesce together and eventually cover the first layer of Si substrate surface. Subsequently, for the second layer, AlN species undergo the nucleation on the first layer, small islands, coalescence, and overall coverage of the second layer on Si substrate. If the first layer is not fully covered, AlN species can jump from the second layer to the first layer due to their highly kinetic energy, which is termed as inter-layer jump[39-41] and promote for the two-dimension growth of AlN films on Si substrate.

CrystEngComm Accepted Manuscript

As the layer-by-layer growth continues, the AlN film thickness gradually increases. Due to large -18.9 % lattice mismatches between AlN and Si, AlN lattice subjected to tensile strain from Si lattice, leading to mismatch stress in AlN/Si (111) interface during the growth. In order to release the mismatch stress, misfit dislocations generate in the interface. As the film thickness gradually increases, these misfit dislocations will propagate and stretch upwards, resulting in the formation of threading dislocations. AlN film growing on Si (111) substrates by PLD is two-dimensional layer-by-layer growth regime in relation to strain-relaxation mechanism.

In short, energetic AlN species arrive at Si substrate surface, and then undergo the nucleation, formation of small islands, coalescence of large islands, and overall coverage of Si substrate surface. Eventually, AlN film forms on Si substrate layer by layer, which is related with the highly energetic effect, the pulsed effect and the strain-relaxation mechanism.

5. Conclusions

In summary, we have comprehensively proposed the epitaxial growth mechanism and dislocations formation causes of AlN films on Si (111) substrates by PLD. Due to the highly energetic effect and pulsed effect of PLD, the epitaxial process of AlN film growing on Si (111) by PLD is two-dimensional layer-by-layer growth regime in relation to strain-relaxation mechanisms. At the optimum growth conditions, it exhibits a 1.5 nm-thick single-crystalline AlN layer rather than an amorphous SiN_x layer, which is attributed to the fact that the pre-ablation of AlN targets can eventually inhibit Si-N interfacial reaction. Whereas, severely interfacial reaction and an AlSiN layer were found in the AlN/Si (111) interface in non-optimal growth conditions, which is derived from the interfacial interdiffusion and penetration between active Si atoms and AlN species. The schematic of epitaxial process of AlN films on Si (111) substrates can be categorized into three sub-stages, in which AlN, Al and N etc. species are created by laser, expand into a nitrogen background, arrive at Si substrate surface, and forms AlN film layer by layer.

We believe the comprehensive investigation on the epitaxial growth mechanism and dislocations formation causes of AlN films on Si (111) substrates by PLD is an essential theoretical basis for growing high-quality AlN single-crystalline films and fabricating AlN-based devices, particularly for acoustic filters where abrupt heterointerfaces with substrates and high-quality AlN films are highly desired.

CrystEngComm Accepted Manuscript

Acknowledgements

The authors gratefully acknowledge financial supports from National Science Foundation of China (Contract Nos. 51002052, 51372001), Excellent Youth Foundation of Guangdong Scientific Committee (Contract No. S2013050013882), Key Project in Science and Technology of Guangdong Province (Contract No. 2011A080801018), and Strategic Special Funds for LEDs of Guangdong Province (Contracts No. 2011A081301010, and 2011A081301012).

References

1 R. R. Sumathi, *CrystEngComm*, 2013, **15**, 2232.

2 L. C. Xu, R. Z. Wang, X. D. Yang, and H. Yan, *J. Appl. Phys.*, 2011, **110**, 043528.

3 D. Zhu, D. J. Wallis and C. J. Humphreys, *Rep. Prog. Phys.*, 2013, **76**,106501

4 Y. Taniyasu, M. Kasu, and T. Makimoto. *Nature*, 2006, **441**, 325.

5 H. Lee, K. H. Yoon, and J. K. Lee, *J. Appl. Phys.*, 2002, **92**, 4062.

6 H. Amano, N. Sawaki, I. Akasaki, and Y. Toyoda, *Appl. Phys. Lett.*, 1986, **48**, 353.

7 A.T. Schremer, J. A. Smart, Y. Wang, O. Ambacher, N. C. MacDonald, and J. R. Shealy, *Appl. Phys. Lett.*, 2000, **76**, 736.

8 F. Semond, P. Lorenzini, N. Grandjean, and J. Massies, *Appl. Phys. Lett.*, 2001, **78**, 335.

9 U. Rössner, J. L. Rouviere, A. Bourret, and A. Barski, *Mater. Res. Soc. Symp. Proc.*, 1996, **395**, 145.

10 A. Bourret, A. Barski, J. L. Rouvière, G. Renaud, and A. Barbier, *J. Appl. Phys.*, 1998, **83**, 2003.

11 J. Li, J. Y. Lin, and H. X. Jiang, *Appl. Phys. Lett.*, 2006, **88**, 171909.

12 G. W. Auner, F. Jin, V. M. Naik, and R. Naik, *J. Appl. Phys.*, 1999, **85**, 7879.

13 Z. M. Ren, Y. F. Lu, H. Q. Ni, T. Y. F. Liew, B. A. Cheong, S. K. Chow, M. L. Ng, and J. P. Wang, *J. Appl. Phys.*, 2000, **88**, 7346.

14 G. Li, and H. Yang, *Cryst. Growth & Design*, 2011, **11(3)**, 664.

15 M. N. R. Ashfold, F. Claeyssens, G. M. Fuge and S. J. Henley, *Chem. Soc. Rev.*, 2004, **33**, 23.

16 D. Marla, U. V. Bhandarkar, and S. S. Joshi. *J. Appl. Phys.*, 2011, **109**, 021101.

17 R. K. Singh, W. Holl, and J. Narayan. *J. Appl. Phys.*, 1990, **68**, 233.

18 Z. Chen, and A. Bogaerts. *J. Appl. Phys.*, 2005, **97**, 063305.

19 A. Bogaerts, Z. Chen, R. Gijbels, and A. Vertesb. *Spectrochim. Acta B*, 2003, **58**, 1867.

CrystEngComm Accepted Manuscript

20 R. Rozman, I. Grabec, and E. Govekar. *Appl. Surf. Sci*., 2008, **254**, 3295.

21 M. Aghaei, S. Mehrabian, and S. H. Tavassoli. *J. Appl. Phy*s., 2008, **104**, 053303.

22 S. Bakalova, A. Szekeres, A. Czirakib, C. P. Lungu, S. Grigorescu, G. Socol, E. Axente, and I. N. Mihailescu. *Appl. Surf. Sci.*, 2007, **253**, 8215.

23 R. D. Vispute, J. Narayan, H. Wu, and K. Jagannadham. *J. Appl. Phys*., 1995, **77(9)**, 4724

24 A. Bourret, A. Barski, J. L. Rouviere, G. Renaud, and A. Barbier. *J. Appl. Phys*., 1998, **83**, 2003.

25 G. W. Auner, and F. Jin, V. M. Naik, and R. Naik. *J. Appl. Phys*., 1999, **85**, 7879

26 H. Yang, W. Wang, Z. Liu, and G. Li. *CryEngComm*., 2013, **15**, 7171.

27 V. Lebedev, V. Cimalla, U. Kaiser, Ch. Foerster, J. Pezoldt, J. Biskupek, and O. Ambacher. *J. Appl. Phys*., 2005, **97,** 114306.

28 G. Radtke, M. Couillard, G. A. Botton, D. Zhu, and C. J. Humphreys, *Appl. Phys. Lett.*, 2010, **97**, 251901

29 G. Radtke, M. Couillard, G. A. Botton, D. Zhu, and C. J. Humphreys, *Appl. Phys. Lett.*, 2012, **100**, 011910

30 Z. M. Ren, Y. F. Lu, and H. Q. Ni. *J. Appl. Phys.*, 2000, **88**, 7346.

31 D. J. Xi, Y. D. Zheng, P. Chen, Z. M. Zhao, P. Chen, S.Y. Xie, R. L. Jiang, B. Shen, S. L. Gu and R. Zhang. *Chin. Phys. Lett.*, 2002, **19**, 543.

32 Y. Hirayama, H. Yabe, and M. Obara. *J. Appl. Phys.*, 2001, **89**, 2943.

33 E. Gyorgy, C. Ristoscu, I. N. Mihailescu, A. Klini, N. Vainos, C. Fotakis, C. Ghica, G. Schmerber, and J. Faerber. *J. Appl. Phys*., 2001, **90**, 456.

34 C. Ristoscu, I. N. Mihailescu, M. Velegrakis, M. Massaouti, A. Klini, and C. Fotakis. *J. Appl. Phys*., 2003, **93**, 2244.

35 A. Santagata, V. Marotta, S. Orlando, R. Teghil, M. Zaccagnino, and A. Giardini. *Appl.Surf. Sci.*, 2003, **208**, 101.

36 C. Chu, P. P. Ong, H. F. Chen, and H. H. Teo. *Appl. Surf. Sci*., 1999, **137**, 91.

37 B. Eliasson. *IEEE Trans. Plasma Sci.*, 1991, **19**, 1063.

38 J. H. Park, E. Pfender, and C. H. Chang. *Plasma Chem. Plasma Process*., 2000, **20**, 165.

39 R. L. Schwoebel. *J. Appl. Phys.*, 1969, **40**, 614.

40 N. A. Levanov, V. S. Stepanyuk, and W. Hergert. *Phys. Rev. B*, 2000, **61**, 2230.

41 G. Koster, G. J. H. M. Rijnders, D. H. A. Blank, and H. Rogalla. *Appl. Phys. Lett.*, 1999, **74**, 3729.

CrystEngComm Accepted Manuscript

42 D. H. A. Blank, G. Koster, G. A. Rijnders, E. Setten, P. Slycke, and H. Rogalla. *J. Cryst. Growth*, 2000, **211**, 98.

43 P. O. Jubert, O. Fruchart, and C. Meyer. *Surf. Sci.*, 2003, **522**, 8.

44 J. Shen, G. Zheng, and J. Kirschner. *Surf. Sci. Reports*, 2004, **52**, 163.

45 X. H. Xu, R. Q. Zhang, X. Z. Dong, and G. A. Gehring. *Thin Solid Films*, 2006, **515**, 2754.

CrystEngComm Accepted Manuscript

Figure captions

FIG. 1. The XRD analysis of AlN/ Si (111) films, (a) The typical ω-2θ scan, (b) FWHMs of the AlN (0002) and AlN (10-12) XRD rocking curves of AlN grown for 30 min as a function of nitrogen plasma pressure

FIG. 2. The SEM images of AlN/ Si(111) films grown at different pressures, (a) 4×10^{-4} Torr, (b) 1×10^{-3} Torr, (c) 4×10^{-3} Torr, (d) 8×10^{-3} Torr, (e) 1.2×10^{-2} Torr, and (f) EDS line-scan analysis for AlN/ Si (111) film grown at 4×10^{-4} Torr

FIG. 3. The TEM images of AlN/Si (111) films grown at (a) 1×10^{-3} Torr, (b) 8×10^{-3} Torr

FIG. 4. The HRTEM images of AlN/Si (111) interfaces grown at (a) 1×10^{-3} Torr, (b) 8×10^{-3} Torr

FIG. 5. The SAED images of AlN/Si (111) films grown at (a) 1×10^{-3} Torr, (b) 8×10^{-3} Torr, in which the spots marked in red correspond to planes of Si, and the spots marked in white correspond to planes of AlN.

CrystEngComm Accepted Manuscript

FIG. 1.

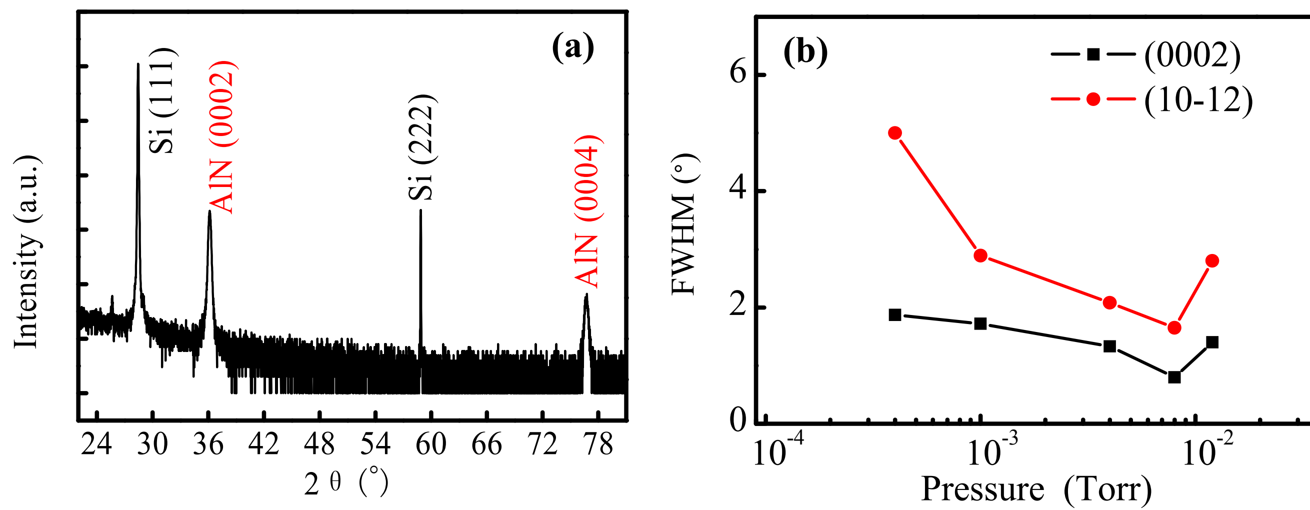

CrystEngComm Accepted Manuscript

FIG. 2.

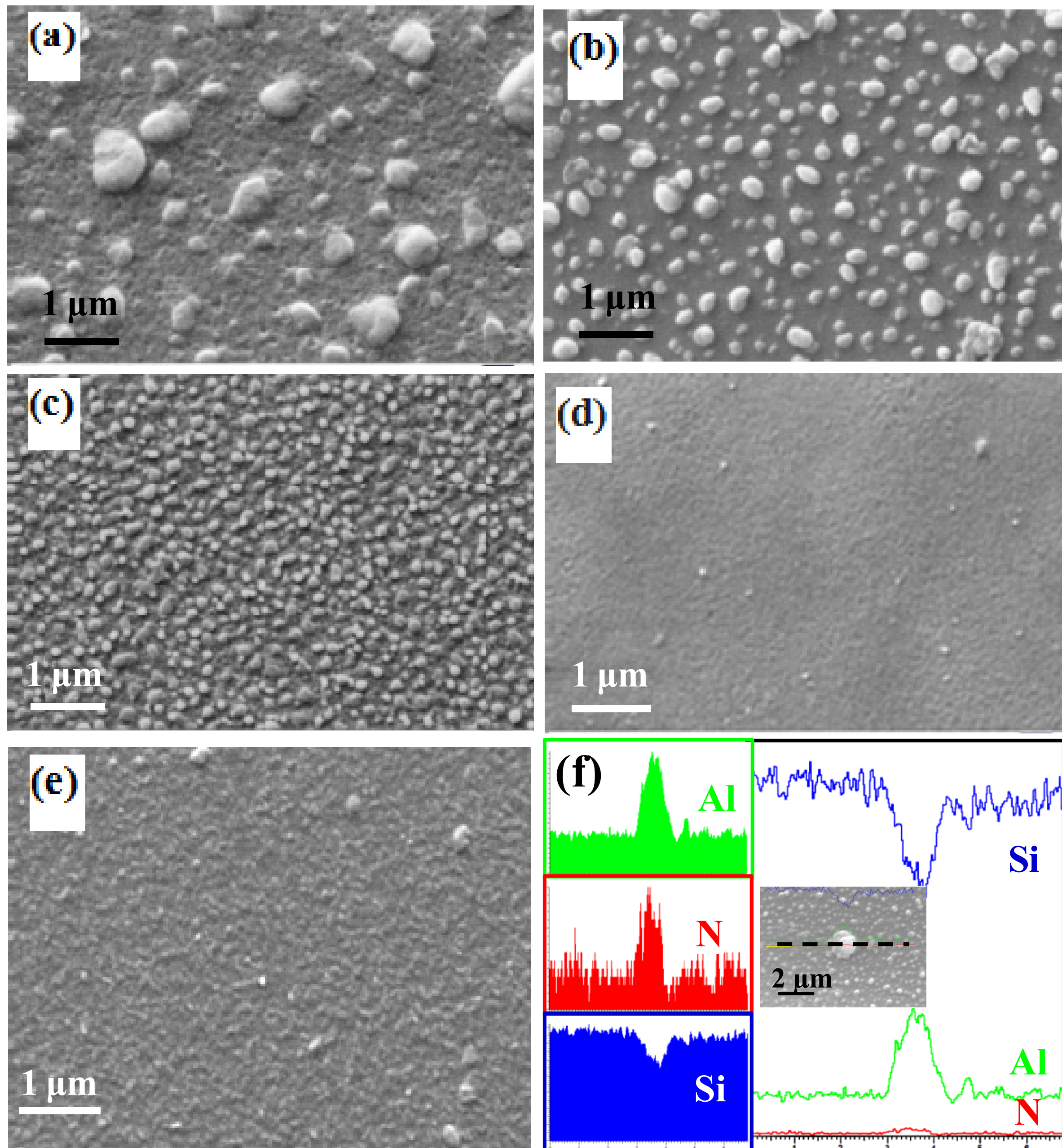

CrystEngComm Accepted Manuscript

FIG. 3.

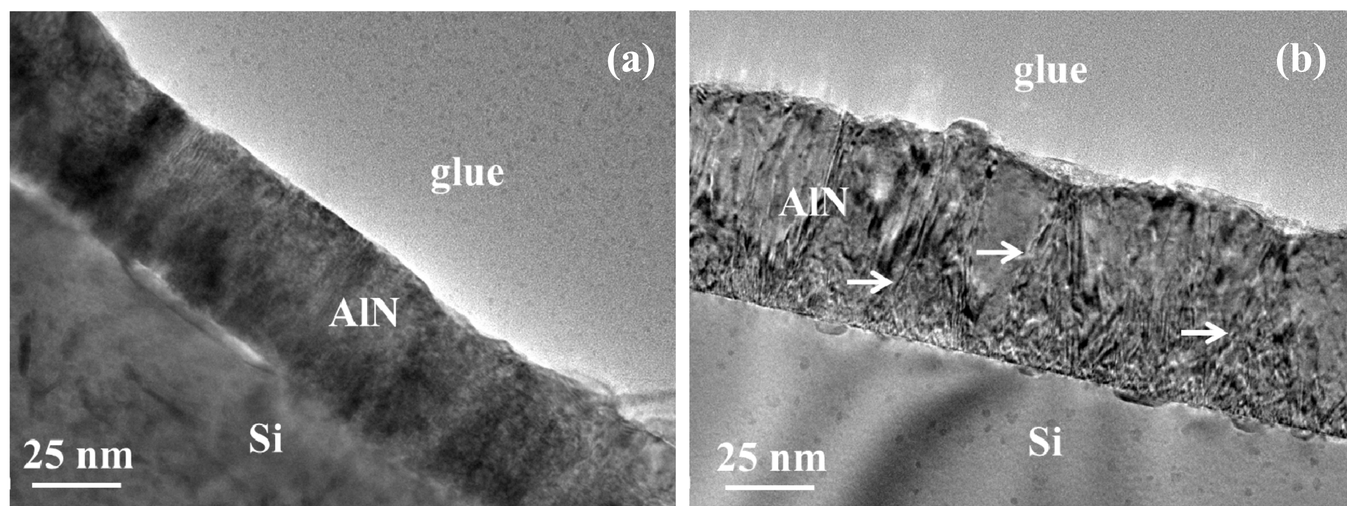

CrystEngComm Accepted Manuscript

FIG. 4.

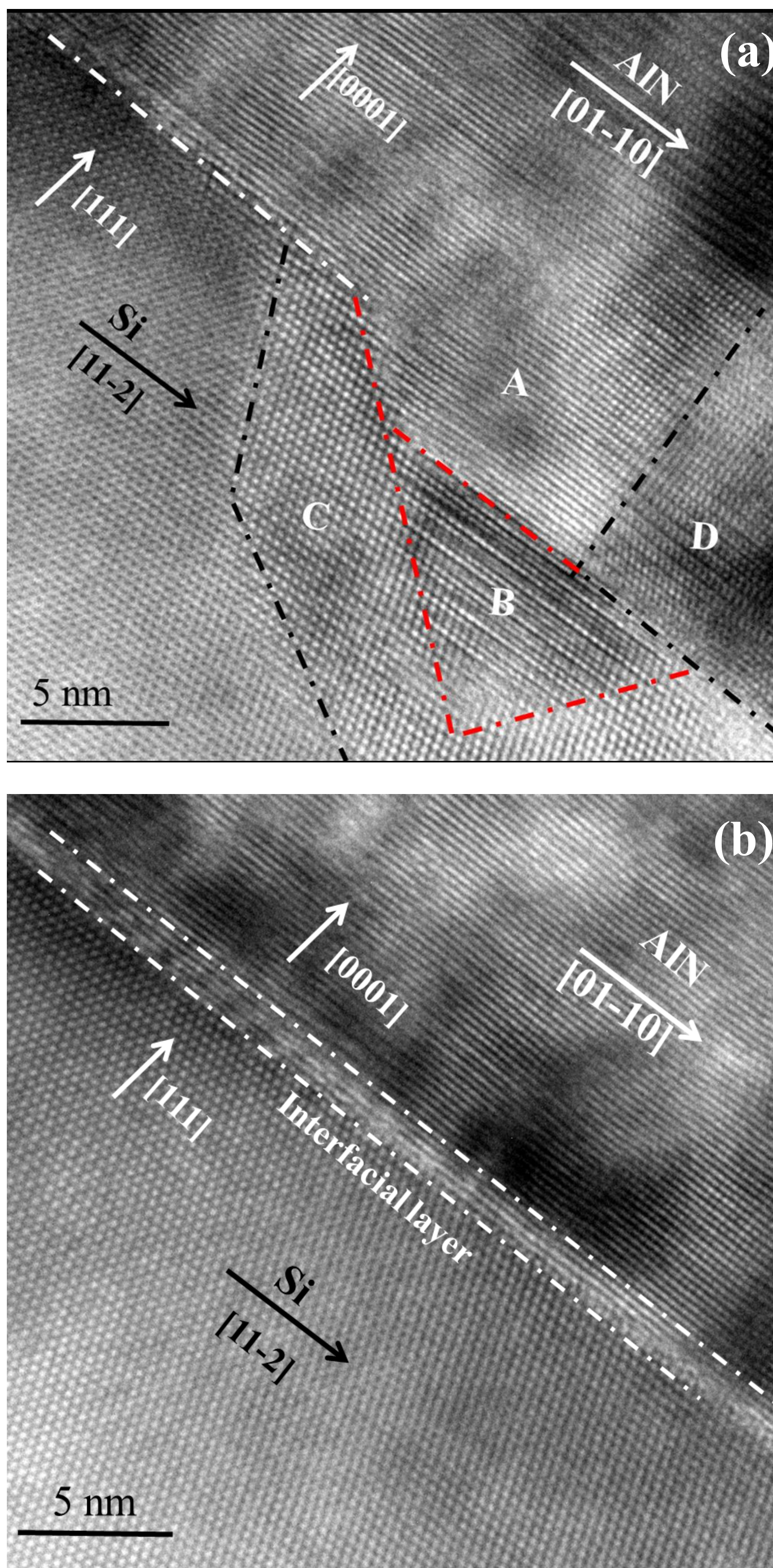

CrystEngComm Accepted Manuscript

FIG. 5.

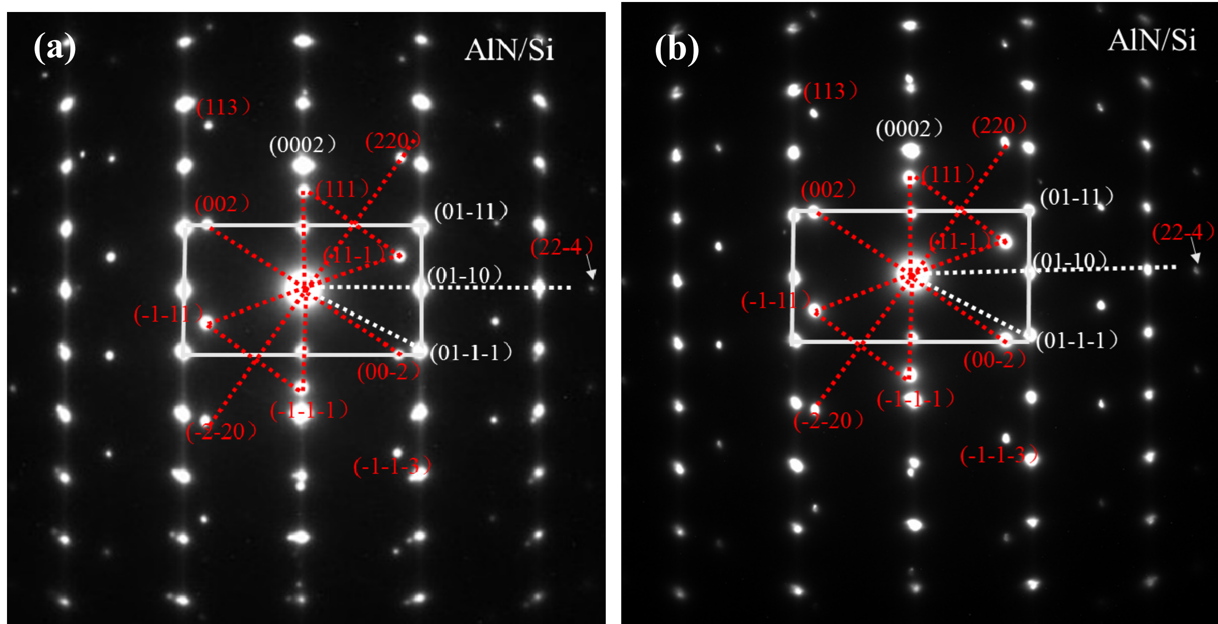

CrystEngComm Accepted Manuscript